



Published in final edited form as:

*Cancer Immunol Res.* 2018 September ; 6(9): 1100–1109. doi:10.1158/2326-6066.CIR-17-0405.

## Reducing *Ex Vivo* Culture Improves the Antileukemic Activity of Chimeric Antigen Receptor (CAR) T Cells

Saba Ghassemi<sup>1,2</sup>, Selene Nunez-Cruz<sup>1,2</sup>, Roddy S. O'Connor<sup>1,2,3</sup>, Joseph A. Fraietta<sup>1,2,3</sup>, Prachi R. Patel<sup>1,2</sup>, John Scholler<sup>1,2</sup>, David M. Barrett<sup>4</sup>, Stefan M. Lundh<sup>1</sup>, Megan M. Davis<sup>1,2</sup>, Felipe Bedoya<sup>1,2</sup>, Changfeng Zhang<sup>1</sup>, John Leferovich<sup>1,2</sup>, Simon F. Lacey<sup>1,2</sup>, Bruce L. Levine<sup>1,2</sup>, Stephan A. Grupp<sup>4</sup>, Carl H. June<sup>1,2,3</sup>, J. Joseph Melenhorst<sup>#1,2</sup>, Michael C. Milone<sup>#1,2</sup>

<sup>1</sup>Center for Cellular Immunotherapies, Perelman School of Medicine, University of Pennsylvania, Philadelphia, Pennsylvania.

<sup>2</sup>Department of Pathology and Laboratory Medicine, Perelman School of Medicine, University of Pennsylvania, Philadelphia, Pennsylvania.

<sup>3</sup>Parker Institute for Cancer Immunotherapy, University of Pennsylvania, Philadelphia, Pennsylvania.

<sup>4</sup>Division of Oncology, The Children's Hospital of Philadelphia, Philadelphia, Pennsylvania.

# These authors contributed equally to this work.

### Abstract

The success of chimeric antigen receptor (CAR)-mediated immunotherapy in acute lymphoblastic leukemia (ALL) highlights the potential of T-cell therapies with directed cytotoxicity against

---

**Corresponding Authors:** Michael C. Milone, Perelman School of Medicine at the University of Pennsylvania, 3400 Spruce Street 7103 Founders Pavilion, Philadelphia, PA 19104. Phone: 215-662-6575; Fax: 215-662-7529, milone@pennmedicine.upenn.edu; and Saba Ghassemi, ghassemi@pennmedicine.upenn.edu.

J.J. Melenhorst and M.C. Milone contributed equally to this article.

Authors' Contributions

**Conception and design:** S. Ghassemi, J.A. Fraietta, J. Scholler, S.M. Lundh, F. Bedoya, S.A. Grupp, J.J. Melenhorst, M.C. Milone

**Development of methodology:** S. Ghassemi, J. Scholler, F. Bedoya, S.A. Grupp, J.J. Melenhorst, M.C. Milone

**Acquisition of data (provided animals, acquired and managed patients, provided facilities, etc.):** S. Ghassemi, S. Nunez-Cruz, R.S. O'Connor, P.R. Patel, D.M. Barrett, S.M. Lundh, F. Bedoya, J. Leferovich, S.F. Lacey

**Analysis and interpretation of data (e.g., statistical analysis, biostatistics, computational analysis):** S. Ghassemi, S. Nunez-Cruz, J.A. Fraietta, P.R. Patel, J. Scholler, D.M. Barrett, S.M. Lundh, F. Bedoya, S.A. Grupp, J.J. Melenhorst, M.C. Milone

**Writing, review, and/or revision of the manuscript:** S. Ghassemi, S. Nunez-Cruz, R.S. O'Connor, J.A. Fraietta, P.R. Patel, D.M. Barrett, M.M. Davis, F. Bedoya, B.L. Levine, S.A. Grupp, C.H. June, J.J. Melenhorst, M.C. Milone

**Administrative, technical, or material support (i.e., reporting or organizing data, constructing databases):** S. Ghassemi, S. Nunez-Cruz, S.F. Lacey, S.A. Grupp

**Study supervision:** S. Ghassemi, S. Nunez-Cruz, D.M. Barrett, J.J. Melenhorst, M.C. Milone

**Other (in vivo data acquisition):** J. Leferovich

Disclosure of Potential Conflicts of Interest

S.F. Lacey reports receiving commercial research funding from Tmunity and Novartis. B.L. Levine reports receiving commercial research funding from Novartis and Tmunity; has an ownership interest in University of Pennsylvania and Tmunity; and is a consultant/advisory board member for Incysus, BrammerBio, CRC Oncology, and Cure Genetics. S.A. Grupp reports receiving commercial research funding from and is a consultant/advisory board member for Novartis. C.H. June reports receiving commercial research funding from Tmunity and has an ownership interest in an IP licensed to Novartis. M.C. Milone reports receiving commercial research funding from Novartis. No potential conflicts of interest were disclosed by the other authors.

**Note:** Supplementary data for this article are available at Cancer Immunology Research Online (<http://cancerimmunolres.aacrjournals.org/>).

specific tumor antigens. The efficacy of CAR T-cell therapy depends on the engraftment and persistence of T cells following adoptive transfer. Most protocols for T-cell engineering routinely expand T cells *ex vivo* for 9 to 14 days. Because the potential for engraftment and persistence is related to the state of T-cell differentiation, we hypothesized that reducing the duration of *ex vivo* culture would limit differentiation and enhance the efficacy of CAR T-cell therapy. We demonstrated that T cells with a CAR-targeting CD19 (CART19) exhibited less differentiation and enhanced effector function *in vitro* when harvested from cultures at earlier (day 3 or 5) compared with later (day 9) timepoints. We then compared the therapeutic potential of early versus late harvested CART19 in a murine xenograft model of ALL and showed that the antileukemic activity inversely correlated with *ex vivo* culture time: day 3 harvested cells showed robust tumor control despite using a 6-fold lower dose of CART19, whereas day 9 cells failed to control leukemia at limited cell doses. We also demonstrated the feasibility of an abbreviated culture in a large-scale current good manufacturing practice-compliant process. Limiting the interval between T-cell isolation and CAR treatment is critical for patients with rapidly progressing disease. Generating CAR T cells in less time also improves potency, which is central to the effectiveness of these therapies.

---

## Introduction

Adoptive T-cell immunotherapy using genetically engineered T cells with chimeric antigen receptors (CAR) or T-cell receptors (TCR) is capable of inducing dramatic antitumor responses in patients with hematologic malignancies (1–10). T-cell therapy also shows promise in the solid tumor setting (11–15). Despite the high overall rate of complete response to CD19-specific CAR therapy in acute lymphoblastic leukemia (ALL), some patients still relapse due to premature loss of the engineered T cells (4). T-cell engraftment following adoptive transfer is also associated with both the depth and the duration of clinical response (6, 16, 17). The mechanism(s) that underlie the observed variation in engraftment are unclear.

The state of T-cell differentiation influences the engraftment and persistence of T cells following adoptive transfer. Naïve and memory T cells appear to have the greatest potential for engraftment (18–21). Cultured T cells derived from less differentiated memory T-cell pools also support improved engraftment and persistence following adoptive transfer in both tumor and infectious disease models (19, 22–25) and human patients (26). Cultures established using stem cell memory (T<sub>scm</sub>), central memory (T<sub>cm</sub>), and naïve-like T cells exhibit fewer effector differentiated T cells compared with cultures using effector memory T cells (T<sub>em</sub>; refs. 19, 24). These data suggest a model in which T cells undergo progressive differentiation during *ex vivo* culture that is associated with reduced persistence following adoptive transfer (27). Maintenance of the less differentiated state is poorly understood but likely depends upon soluble factors, as well as cell–cell interactions found within unique tissue microenvironments, the so-called “memory niche” that cannot be fully recapitulated *ex vivo* or in humanized mouse models (28–31).

We hypothesized that extensive *ex vivo* culture of T cells, although amplifying T-cell numbers, also leads to significant loss of “stemness” that limits engraftment and persistence

following adoptive transfer. In addition to potentially reducing the therapeutic effectiveness of these cells, cellular manufacturing processes involving extended *ex vivo* culture also increase the labor and material costs of manufacturing of T-cell immunotherapies, which creates a barrier to bringing T-cell immunotherapies to patients.

Using a T-cell culture platform based upon bead-immobilized CD3 and CD28 agonist antibodies, we showed that minimally *ex vivo*-expanded T cells were functionally superior for adoptive T-cell immunotherapy of leukemia. The beneficial effects of reduced culture duration were manifested in improved *in vitro* proliferation and effector function. This improved *in vitro* function of minimally cultured CAR T cells was directly correlated with improved engraftment and antitumor function *in vivo*, which led to rejection of human ALL in a xenograft model, even at a 6-fold lower dose. Our results suggest that prolonged *ex vivo* culture may be counterproductive, leading to greater numbers of T cells at the expense of reduced long-term persistence that is necessary for durable antitumor responses. We provide evidence that abridged large-scale T-cell cultures are feasible for both liquid and solid tumor indications.

## Materials and Methods

### Generation of CAR constructs

The CD19-BB $\zeta$  CAR consisting of a CD8 hinge, 4-1BB costimulatory domain, and CD3 $\zeta$  signaling domain was generated as previously described (32). This is the same construct used in CTL019 trials at the University of Pennsylvania (33). The mesothelin (Meso)-BB $\zeta$  CAR having a CD8 hinge, 4-1BB costimulatory domain, and CD3 $\zeta$  signaling domain was generated as previously described (34).

### Cells and cell cultures

Cells from ALL ( $n = 36$ ), chronic lymphocytic leukemia (CLL) ( $n = 3$ ), and ovarian cancer ( $n = 3$ ) subjects enrolled in CAR T-cell clinical studies at the University of Pennsylvania ([clinicaltrials.gov](https://clinicaltrials.gov) NCT#s: [NCT02030847](https://clinicaltrials.gov/ct2/show/study/NCT02030847), [NCT00891215](https://clinicaltrials.gov/ct2/show/study/NCT00891215), and [NCT02159716](https://clinicaltrials.gov/ct2/show/study/NCT02159716)) were collected after informed consent under institutional review board (IRB)-approved protocols at the University of Pennsylvania. Human cells were obtained from peripheral blood of patients by apheresis after written informed consent under protocols approved by the IRB of the University of Pennsylvania in accordance with the U.S. Common Rule. T cells were purified by negative selection using the RosetteSep T cell enrichment Cocktail. Peripheral blood leukocytes from healthy donors were obtained from the Human Immunology Core. Following isolation, T cells were cultured in X-VIVO 15 (Cambrex) supplemented with 5% normal human AB serum (Valley Biomedical), 2 mmol/L L-glutamine (Cambrex), 20 mmol/L HEPES (Cambrex), and IL2 (100 units/mL; R&D Systems). Stimulation and culture conditions were done exactly like in our clinical test expansions for the CTL019 trials (33). Fresh or cryopreserved donor and patient cells were stimulated with magnetic beads precoated with agonist antibodies against CD3 and CD28 (Life Technologies) at a ratio of three beads per cell, and then resuspended at a concentration of  $10^6$  T cells/mL for expansion. T cells were then lentivirally transduced with CD19-BB $\zeta$  CAR at day 1 and expanded for 9 days or harvested at specific timepoints for analysis. Cells were maintained

in culture at a concentration of  $0.5 \times 10^6$  cells/mL by adjusting the concentration every other day based on counting by flow cytometry using countbright beads (BD Bioscience) and monoclonal antibodies to human CD4 (clone OKT4) and CD8 (clone SK1; ref. 35). Cell volume was also measured with a Multisizer III particle counter (Beckman-Coulter) every other day.

In the clinical current good manufacturing practice (cGMP) large-scale studies, cryopreserved patient lymphocytes were thawed, washed, and resuspended in the medium described above. The washed products were split into two cultures, designated for day 5 and 9 cultures, respectively. These cultures were seeded into gas-permeable flasks (Baxter Oncology). Magnetic beads with conjugated anti-CD3 (OKT3; Ortho Biotech) and anti-CD28 (clone 9.3; Bio X Cell) were added at a 3:1 bead/CD3<sup>+</sup> cell ratio. Day 5 cultures were transduced with the Meso-BB $\zeta$  CAR lentiviral vector on day 1, whereas the day 9 cultures were transduced on days 0 and 1. Both cultures were washed on day 3 to eliminate residual vector. Viability and concentration were determined by flow cytometry. Cells were then maintained in culture at a concentration of  $0.5 \times 10^6$  cells/mL. On day 5, the day 5 cultures were harvested, and day 9 cultures were transferred to a Wave Bioreactor and maintained for 4 more days prior to harvest. After completion of cell culture, the magnetic beads were removed tested for release criteria specified for T-cell phenotype, cell viability ( > 70%), concentration ( > 80% CD3<sup>+</sup>CD45<sup>+</sup>), and transduction efficiency ( > 2%).

All cell lines (NALM-6, K562, and HEK293T cell) were originally obtained from the American Type Culture Collection (ATCC). K562 cells were transduced with a lentiviral vector encoding human CD19 (K562-CD19). Alternatively, K562 cells were engineered to constitutively express click beetle green luciferase/enhanced GFP as well as mesothelin. Cells were expanded in RPMI medium containing 10% FBS, penicillin, and streptomycin at a low passage and tested for mycoplasma using the MycoAlert detection Kit according to the manufacturer's instructions (Lonza). Cell line authentication was performed by the University of Arizona Genetics Core based on criteria established by the International Cell Line Authentication Committee. Short tandem repeat profiling revealed that these cell lines were above the 80% match threshold.

### Flow cytometry

At harvest or upon thawing,  $1 \times 10^6$  cells were stained for cell surface markers to analyze T-cell differentiation status. The following pretitrated antibodies were used: anti-CCR7-FITC (clone 150503; BD Pharmingen); anti-CD45RO-PE (clone UCHL1), anti-CD8-H7APC (clone SK1; BD Biosciences); anti-CD95-PerCP-Cy5.5 (Clone DX2), anti-CD4-BV510 (clone OKT4), anti-CD3-BV605 (clone OKT3), anti-CD14-Pacific Blue (PB; clone HCD14), anti-CD19-PB (clone HIB19; BioLegend); anti-CD27-PE-Cy7 (clone 1A4CD27; Beckman Coulter); and carboxyfluorescein diacetate succinimidyl ester (CFSE) and ViViD (Invitrogen). The anti-CAR19 idiotype for surface expression of CAR19 was provided by Novartis (Basel, Switzerland).

Cells were washed with PBS and stained for viability using LIVE/DEAD Fixable Violet (Molecular Probes) for 15 minutes, washed once, and resuspended in fluorescence-activated cell sorting (FACS) buffer consisting of PBS, 1% BSA, and 5 mmol/L

ethylenediaminetetraacetic acid (EDTA). Cells were then incubated with the above indicated antibodies for 1 hour at 4°C. Sample were then washed 3 times with FACS buffer and fixed in 1% paraformaldehyde. Positively stained cells were differentiated from background using fluorescence-minus-one controls. Flow cytometry was performed on BD LSR Fortessa. Analysis was performed using Flowjo software (Tree Star Inc. version 10.1).

### Proliferation and cytokine secretion

Proliferation was quantified with a CFSE dilution assay. T cells were washed and stained with 1  $\mu\text{mol/L}$  CFSE (Life Technologies) for 3.5 minutes at room temperature. The reaction was quenched by adding PBS with 10% FBS and washed twice with same buffer. Cells were then incubated at a ratio of 1:1 with irradiated target cells (K562-CD19 vs. K562-wild type) for 120 hours in a cytokine-free media. Live CD3<sup>+</sup> cells were then enumerated using bead-based flow cytometry as previously described (32). The fold change of live T cells was calculated relative to the live T-cell count at day 0. Supernatants were also collected at 24 hours to assess cytokine production. Measurement of Cytokine was performed with a Luminex bead array platform (Life Technologies) according to the manufacturer's instructions. All samples were analyzed in triplicate and compared against multiple internal standards with a 9-point standard curve. Data were acquired on a FlexMAP-3D system (Luminex), and analysis was performed in XPonent 4.0 software (Luminex), as well as through five-parameter logistic regression (4).

### Cytotoxicity assays

The ability of CART19 cells (T cells engineered with the CD19-BB $\zeta$  CAR) to kill target cells expressing CD19 was evaluated using a <sup>51</sup>Cr release assay. Note that  $5 \times 10^5$  K562-CD19 target cells, K562-wild type control cells, and NALM6 leukemia cells were labeled with 50  $\mu\text{L}$  of Na<sub>2</sub><sup>51</sup>CrO<sub>4</sub> (PerkinElmer) for 90 minutes, washed twice in PBS, and resuspended in phenol red-free medium (Gibco) with 5% FBS. T cells were then incubated with loaded target cells for 4 or 20 hours at various effector:target (E:T) ratios. Chromium release into the supernatant, as a measure of target cell killing, was measured with a liquid scintillation counter (MicroBeta triluX, PerkinElmer). Target cells incubated in medium alone or with 1% SDS were used to determine spontaneous (S) or maximum (M) <sup>51</sup>Cr release. Percentage of specific lysis was calculated as follows:  $100 \times (\text{cpm experimental release} - \text{cpm S release}) / (\text{cpm M release} - \text{cpm S release})$ .

CART-meso cells (T cells containing the Meso-BB $\zeta$  CAR) from patients were cocultured with mesothelin-expressing target cells. Cellular supernatants were collected after 24 hours of stimulation. The ability of mesothelin-specific CAR T cells to kill tumor targets was tested in a 16-hour luciferase-based cytotoxicity assay. K562 cells engineered to stably express mesothelin and firefly luciferase (K562-meso-luc) were cocultured with CART-meso cells or donor-matched untransduced T cells at the indicated E:T ratios in 96-well round-bottom plates at a total volume of 200  $\mu\text{L}$ . Target cells alone were seeded in parallel at the same density to quantify the maximum luciferase expression (relative luminescent units; RLU<sub>max</sub>). Following coculture, 100  $\mu\text{L}$  of supernatant was removed, and 100  $\mu\text{L}$  of luciferase substrate (Bright-Glo; Promega) was added to the remaining supernatant and cells. Luminescence was measured after a 10-minute incubation using the EnVision (PerkinElmer)

plate reader. The percent cell lysis was obtained using the following calculation:  $[1 - (\text{RLU}_{\text{experimental}}/\text{RLU}_{\text{max}})] \times 100$ . Two replicate experiments were done, and each was performed in triplicate.

### Quantitative PCR analysis

CAR T cells were harvested, and genomic DNA was isolated. Using 200 ng genomic DNA, qPCR analysis was performed to detect the integrated BB $\zeta$  CAR transgene sequence using ABI Taqman technology as described in refs. 3, 32. To determine copy number per unit DNA, an 8-point standard curve was generated consisting of 5 to 106 copies of the BB $\zeta$  lentivirus plasmid spiked into 100 ng nontransduced control genomic DNA. The number of copies of plasmid present in the standard curve was verified using digital qPCR with the same CAR primer/probe set and performed on a QuantStudio<sup>TM</sup> 3D digital PCR instrument (Life Technologies). A CDKN1A-specific primer probe set was used as a normalization control. Each datapoint (sample, standard curve) was evaluated in triplicate with a positive  $C_t$  value in 3/3 replicates with % CV < 0.95% for all quantifiable values.

### *In vivo* models

Axenograft model was used as previously reported (32). Briefly, 6- to 10-week-old NOD-SCID  $\gamma_c^{-/-}$  (NSG) mice, which lack an adaptive immune system, were obtained from Jackson Laboratories or bred in-house under a protocol approved by the Institutional Animal Care and Use Committees (IACUC) of the University of Pennsylvania. Animals were assigned in all experiments to treatment/control groups using a randomized approach. Animals were injected i.v. via tail vein with  $10^6$  NALM6 cells (ATCC) in 0.1 mL sterile PBS. CART19 cells or nontransduced (UTD) human T cells were injected via tail vein at the indicated dose in a volume of 200  $\mu$ L of sterile PBS/ $\text{Ca}^{2+}$  5 to 7 days after injection of NALM6. Anesthetized mice were imaged using a Xenogen IVIS Spectrum system (Caliper Life Science) twice a week. Mice were given an i.p. injection of D-luciferin (150 mg/kg; Caliper Life Sciences). Total flux was quantified using Living Image 4.4 (PerkinElmer) by drawing rectangles of identical area around mice, reaching from head to 50% of the tail length. Background bioluminescence was subtracted for each image individually. Peripheral blood was obtained by retro-orbital bleeding in an EDTA-coated tube, and blood was examined immediately for evidence of T-cell engraftment by flow cytometry using BD Trucount (BD Biosciences). Serum was separated from the blood by centrifugation at 1,200 RPM, for 30 minutes at 4°C, and was tested for several human cytokines. Measurement of Cytokine was performed with aLuminex bead array platform (Life Technologies) according to the manufacturer's instructions. Animals were euthanized at the end of the experiment or when they met prespecified endpoints according to the IACUC protocols (before reaching signals higher  $1 \times 10^{11}$  p/s total flux per mouse, or before the disease is too well established to reverse with therapy). All animal studies were approved by the IACUC of the University of Pennsylvania.

### Statistical analysis

The graphs represent the mean value + SD, unless otherwise indicated. A Student *t* test for paired data, Wilcoxon rank-sum test, or a one-way ANOVA was performed using GraphPad Prism version 4.0a (GraphPad Software). Multiple-comparison *post hoc* corrections were

performed using the Neuman–Keuls test. A  $P$  value  $< 0.05$  was considered statistically significant.

## Results

### T cells progressively differentiate over time during *ex vivo* culture

To study primary human T-cell differentiation over time, we used a well-established, multiparametric flow cytometric approach to distinguish naïve-like (CD45RO<sup>-</sup>CCR7<sup>+</sup>), central memory (T<sub>cm</sub>, CD45RO<sup>+</sup>CCR7<sup>+</sup>), effector memory (T<sub>em</sub>, CD45RO<sup>+</sup>CCR7<sup>-</sup>), and effector (T<sub>te</sub>, CD45RO<sup>-</sup>CCR7<sup>-</sup>) T-cell subsets as shown in Fig. 1A (19, 36). In the naïve-like T-cell compartment, stem cell memory T cells (T<sub>scm</sub>) were identified by coexpression of CD27 and CD95, and naïve T cells (T<sub>n</sub>) were defined by the absence of CD95. T cells obtained from the peripheral blood of healthy donors and individuals with ALL show variable proportions of T-cell subsets (Fig. 1B). Characteristics of the ALL subjects are described in Table 1. T cells from individuals with ALL exhibited a significantly greater proportion of effector-differentiated T cells compared with healthy donors, with the T<sub>em</sub> subset representing the majority population (Fig. 1B). T<sub>n</sub> or T<sub>scm</sub> cells comprised a proportionately lower percentage of the total T cells compared with healthy donors (28% vs. 55.1%,  $P < 0.05$ , for T<sub>n</sub>, and 1.8% vs. 5.9%,  $P < 0.05$ , for T<sub>scm</sub>). The increased proportion of more differentiated T cells in ALL apheresis products was expected and may be related to prior chemotherapy that disproportionately affects the naïve subset of T cells in patients with ALL, while sparing memory cells as previously described (37, 38).

Following activation through the TCR/CD3 complex and CD28, T cells entered a phase of rapid proliferation that was associated with progressive differentiation during 9 days of *ex vivo* culture (Fig. 1C). Healthy donor T cells underwent an approximately 30-fold expansion during this 9-day period (Fig. 1D). During this expansion phase, the proportions of both CD8<sup>+</sup> (Fig. 1E; Supplementary Fig. S1) and CD4<sup>+</sup> (Supplementary Fig. S2) T cells underwent a shift from a naïve to a central memory immune phenotype. This increase in T<sub>cm</sub> frequency was associated with an increase in the absolute number of T<sub>cm</sub> cells, whereas T<sub>n</sub> cells and T<sub>em</sub> cells showed a decrease or remained relatively constant over the same period of culture, respectively. Unlike healthy donors, cultures derived from subjects with ALL showed reduced expansion associated with an initial decrease in total viable cell number (Fig. 1F). This decrease in total cells was associated with a decrease in T cells (T<sub>n</sub> or T<sub>te</sub> phenotype). T<sub>cm</sub> cells showed a relative increase in frequency in cultures that was similar to that observed for healthy donors (Fig. 1G; Supplementary Fig. S2). However, the T<sub>em</sub> subset, which was more frequent in ALL at the start of culture, also showed a robust increase, leading to a final T-cell population that was substantially more differentiated compared with healthy donors (Fig. 1H).

### Early-harvested CAR T cells exhibit enhanced effector function and proliferation

Based upon the observed progressive differentiation, we hypothesized that T cells harvested earlier than day 9 would retain greater potency in adoptive transfer. Day 3 (i.e., 72 hours after anti-CD3/CD28 stimulation and 48 hours after lentiviral transduction) was generally the earliest timepoint at which gene transfer could be robustly evaluated. We, therefore,

decided to perform a systematic analysis of T cells harvested at various timepoints beginning at day 3. Using mechanical bead T-cell disruption by repetitive pipetting, we were able to achieve greater than 95% cell recovery from cultures harvested at all timepoints (Supplementary Table S1). As shown in Fig. 2A and B, early-harvested CART19 cells showed consistently enhanced cytolytic function compared with more extensively cultured T cells. Similarly, early-harvested T cells from ALL patients showed significantly enhanced cytolytic activity compared with cells cultured for 9 days (Supplementary Fig. S3). Harvesting at day 3 was more challenging in cultures derived from individuals with ALL due to the reduced cell viability and yield of the culture at early timepoints compared with healthy donors (Fig. 1F). Although T cells harvested at days 3 and 5 showed spontaneous proliferation in the absence of antigen-expressing target cells, early-harvested T cells (days 3 and 5) derived from healthy donors showed significantly enhanced proliferative capacity following antigen exposure (Fig. 2C). T cells from ALL did not show a demonstrable difference in proliferation between day 5 and 9 harvested cells (Fig. 2D).

The ability to produce effector cytokines in response to antigen in T cells derived from healthy donors was also unaffected by time of harvest, with equivalent activation-dependent production of IL2, IFN $\gamma$ , TNF $\alpha$ , GM-CSF, and other inflammatory cytokines (IL1 $\beta$ , IL4, IL5, IL6, IL8, and IL10) observed (Fig. 2E; Supplementary Fig. S4). We also compared basal cytokine production across all timepoints and observed no significant differences. IFN $\gamma$  production was significantly enhanced in CAR T cells generated from ALL/CLL patients at day 5 relative to day 9. Inflammatory cytokines, including IL1 $\beta$ , IL4, IL6, and IL8, were significantly enhanced in early-harvested T cells. A similar trend was observed for IL2, TNF $\alpha$ , and GM-CSF (Supplementary Fig. S3).

The effector function and proliferation of CART19 cells generated from healthy donors and harvested at different timepoints were investigated using the ALL cell line NALM6, as well as primary CLL cells. In general, cytokines and proliferative capacity were higher for day 5 CAR T cells compared with day 9 cells (Supplementary Fig. S5).

### **Early-harvested CAR T cells exhibit enhanced potency and persistence *in vivo***

Using an established and previously described human xenograft model of ALL in NSG mice (39), we evaluated the potency of CART19 cells derived from healthy donors harvested at days 3, 5, or 9 (Fig. 3A). CART19 cells demonstrated antileukemic activity in all treated mice when BLI was compared with mock T-cell-treated mice (Fig. 3B–D). A high dose of T cells ( $3 \times 10^6$  CAR T cells) exhibited durable efficacy in the majority of mice, as expected (Fig. 3B). However, early-harvested cells (days 3 and 5) exhibited superior tumor control compared with cells harvested on day 9. When using a 6-fold lower dose of CART19 cells, the efficacy was lost for cells harvested at day 9 (Fig. 3C; Supplementary Fig. S6). Only the day 3 harvested cells exhibited persistent leukemia control in all mice at the lower  $0.5 \times 10^6$  cell dose (Fig. 3E).

The control of leukemia was associated with improved persistence of T cells, demonstrated by the significantly increased absolute counts of CART19 cells in the peripheral blood of mice treated with early-harvested cells (days 3 and 5) compared with treatment with later harvested cells (Fig. 3F). Measurement of serum cytokines in an independent experiment,



comparing day 5 with day 9 harvested T cells, demonstrated greater production of cytokines *in vivo* by day 5 harvested CART19 cells, which was consistent with their improved antileukemic function (Fig. 3G; Supplementary Fig. S7). In summary, these findings indicated that T cells harvested as early as day 3 from *ex vivo* cultures could produce more potent antitumor activity with >80% fewer T cells.

### **An abbreviated CART-cell culture approach is clinically feasible**

To evaluate the clinical feasibility of an abbreviated culture approach, we performed a comprehensive retrospective analysis on the CAR T-cell product generated from 27 patients undergoing treatment for relapsed/refractory ALL. CART19 cells were manufactured within the University of Pennsylvania cGMP manufacturing facility, using an FDA-compliant process. As seen in Fig. 4A, patient T cells underwent logarithmic expansion in response to bead activation. We next compared several functional parameters at days 3, 5, 7, and 9 of the *ex vivo* expansions. We showed that 70% (19/27) of day 3 products and >80% (22/27) of day 5 products would meet the preexisting day 9 release criteria with respect to dose, viability, and infection efficiency (Fig. 4B and C).

The feasibility of an abbreviated culture approach for cGMP was also confirmed with several patients undergoing treatment for epithelial ovarian cancer. Following bead activation, cells were lentivirally transduced with a CAR-targeting mesothelin (CART-meso) and subsequently expanded within the University of Pennsylvania cGMP manufacturing facility for either 5 or 9 days using an FDA-compliant process. CAR transduction efficiencies were similar in day 5 and 9 T cells (Supplementary Fig. S8). We showed that early-harvested (day 5) CART-meso cells had enhanced antigen-induced IL2, IFN $\gamma$ , TNF $\alpha$ , and GM-CSF secretion and cytotoxic activity compared with day 9 CART-meso cells (Supplementary Fig. S8). Complementing the superior differentiation status observed previously in early-harvested cells (Fig. 1), we showed that CAR T cells harvested at day 5 from clinical-scale cGMP cultures also yielded progeny with a predominantly central memory phenotype. In contrast, day 9 CAR T cells contained a lower proportion of CCR7<sup>+</sup> memory cells, indicating more effector differentiation occurs during their continued *ex vivo* expansion (Supplementary Fig. S8). All of the day 5 cellular products also met existing day 9 release criteria used for CAR T-cell products manufactured within the University of Pennsylvania manufacturing facility, including total T-cell number, viability, and transduction efficiency. In aggregate, these results demonstrated that generating a CAR T-cell product using an abbreviated culture duration is feasible in the clinical cGMP process setting that uses anti-CD3/CD28–stimulating microbeads. Minimally *ex vivo*–manipulated CART-meso cells retained the enhanced tumor-targeting potency we had observed in small scale.

## **Discussion**

*Ex vivo* cell culture, involving the expansion of genetically modified T cells, is an essential part of CAR T-cell–based therapies. CAR T-cell manufacturing methods involving 9 to 14 days of *ex vivo* culture yield large numbers of T cells for adoptive transfer. Because differentiation of the expanded T cells is an important determinant of efficacy and CAR T

cells progressively differentiate over time, we investigated the qualitative features of CAR T cells at early versus late timepoints in the manufacturing process. We showed that culturing cells for a shorter period provided functionally superior T cells. In contrast to CAR T cells grown over 9 days, limiting time in culture enhanced and maintained effector function *in vivo* and preserved the Tscm subset. These features were associated with CAR T cells that exhibit improved engraftment and antileukemic efficacy following adoptive transfer in a well-established preclinical model of ALL.

Data from multiple preclinical immunotherapy models suggest that the ability of T cells to engraft following adoptive transfer is related to their state of differentiation (22–25). Our data are consistent with these studies. We showed that the progressive differentiation that occurs during *ex vivo* culture was associated with reduced long-term engraftment and overall efficacy of adoptively transferred T cells. A number of interventions have been reported to prevent the differentiation that occurs during T-cell expansion, such as blockade of Fas–FasL interactions (40), Akt inhibition (41, 42), or activation of Wnt signaling (19, 43, 44). Although these approaches may limit differentiation, reducing *ex vivo* culture duration, as demonstrated in our study, is both simple and ultimately more cost- and labor-efficient compared with longer duration cultures, which is important to the widespread clinical application of this technology (45).

Our findings are consistent with a stem cell model of T-cell memory previously proposed by Gattinoni and colleagues (19). We failed to observe an increase in the Tscm compartment during *ex vivo* culture. Rather, this population was numerically maintained during the 9-day culture period, but reduced in frequency. As a result, the number of Tscm cells that were adoptively transferred in day 9 products would be proportionally reduced compared with day 3 products, perhaps explaining the reduced long-term engraftment and efficacy of the more extensively cultured products. Methods of marking T cells to track their fate have been described for retroviral vectors (46). Adapting this approach to lentiviral vectors may provide greater insight into the T-cell subsets required for robust and long-term engraftment.

We provide evidence that CART19 cells harvested on day 3 had an enhanced proliferative capacity upon restimulation with their cognate ligand relative to day 9 CART19 cells. Although speculative, day 9 CAR T cells may exhibit diminished proliferative capacity, a characteristic of exhausted T cells, due to prolonged exposure to agonistic anti-CD3/CD28 beads during the culture process. Studies have shown that by shortening the duration of *ex vivo* T-cell stimulation, T cells possess an enhanced ability to proliferate and secrete effector cytokines, as well as have superior antitumor activity (47). Exhausted T cells are also defined by decreased effector function. We showed that extended culture protocols were associated with a progressive loss of functional competency, such that the cytolytic ability of day 9 cells was inferior relative to day 3 cells. The increased proliferative and cytolytic ability observed *in vitro* provided mechanistic insight into the superior antitumor function observed by day 3 cells in mouse models of leukemia. Our findings show that increased effector activity was a function of antigen-dependent stimulation, with no significant differences in basal cytokine levels observed between day 3 and 9 cells. This increase in effector function, although increasing antitumor efficacy, may, therefore, come at a cost of

enhance cytokine release syndrome and neurotoxicity, both well-described complications of CAR T-cell therapy (48).

Although 3-day CAR T-cell manufacturing yields fewer cells for adoptive transfer, we hypothesized that day 3 CAR T cells would outperform day 9 CAR T cells, given their more favorable phenotype. At lower CAR T-cell doses, only day 3 CAR T cells were capable of sustained control of leukemia in the NALM6 xenograft model. This improved leukemia control was associated with day 3 CAR T-cell persistence for at least 6 weeks. Studies of CART19 cells in human clinical trials demonstrate the importance of T-cell persistence in generating durable clinical responses (6). Persistence of CAR T cells in the setting of solid tumors has also been relatively limited (11, 49–51). Persistence in these settings may be more complex and dependent upon additional factors beyond the quality of the T cells, such as an immunosuppressive tumor microenvironment. However, our results suggested that simple adjustments in the *ex vivo* culture process may boost the proliferative capacity, effector function, and persistence of CAR T cells.

Our historic animal studies of CART19 cells (32), as well as data on B-cell maturation antigen–targeted CAR T cells (52), support the principle that a threshold dose of CAR T cells is necessary to achieve engraftment and efficacy analogous to hematopoietic stem cell (HSC) transplantation, where a minimum number of CD34<sup>+</sup> HSCs are required to achieve reliable and durable engraftment. Although there may be a relationship to the total CAR T-cell dose, our extensive clinical experience with CD19-directed CAR T cells derived through conducting multiple trials (i.e., over 100 CLL and ALL patients treated at the University of Pennsylvania) has also demonstrated that a major factor influencing outcome is the frequency of naïve-like T cells within the starting apheresis material used for CAR T-cell manufacturing (53). As our data demonstrated a loss of CAR T-cell potency with culture, a greater number of CAR T cells yielded during a longer culture period would not be expected to improve clinical outcome. Consistent with the clinical observations, we have shown that CAR T cells generated through a shortened manufacturing process contain a greater proportion of stem-like T cells. The ability of reduced-culture CAR T cells to control leukemia at substantially lower numbers supports the apparent increase in stem-like T-cell frequency.

The ability to generate cells with superior therapeutic potential in a shorter time period also has important implications for CAR T-cell manufacturing. Extended culture durations are costly and may be redundant, as a superior product can be generated in as little as 3 days. In addition to reduced labor, the more limited *ex vivo* culture process conserves materials, such as human serum, that represent a limited resource and scarce manufacturing space. Although approaches to culture CAR T cells in serum-free medium are under development, the effectiveness of these T cells has not yet been established. Current FDA guidelines also require replication competent lentivirus/retrovirus testing for culture periods greater than 96 hours after transduction (54). Adopting culture periods shorter than 5 days will avoid the need for this expensive testing. Finally, abbreviated culture durations could lead to a shorter period of time between apheresis collection and reinfusion of T-cell products. This has important implications for treating patients, especially those with rapidly progressive disease (55).

In summary, our results demonstrated that culturing CAR T cells for a shorter duration yields a cellular product with less differentiated T cells, significantly enhanced effector function, and enhanced proliferative capacity. Collectively, these features lead to enhanced antileukemic efficacy *in vivo*. In a retrospective analysis of CAR T cells manufactured within our cGMP facility, we show that cells harvested at day 3 meet the existing day 9 criterion for achieving infusion criteria in 70% of ALL patients, further supporting the feasibility and immediate translational potential of this approach. Minimally cultured T cells, therefore, provide a simple and more cost-effective method for achieving potent CAR T-cell immunotherapy and deserve evaluation in the clinical setting.

## Supplementary Material

Refer to Web version on PubMed Central for supplementary material.

## Acknowledgments

This work was supported by a research agreement with Novartis.

We are grateful to Anthony Secreto and Gwenn Danet for their technical assistance with mouse studies. We would like to thank Fang Chen and Natalka Kengle for their assistance with cytokine assays.

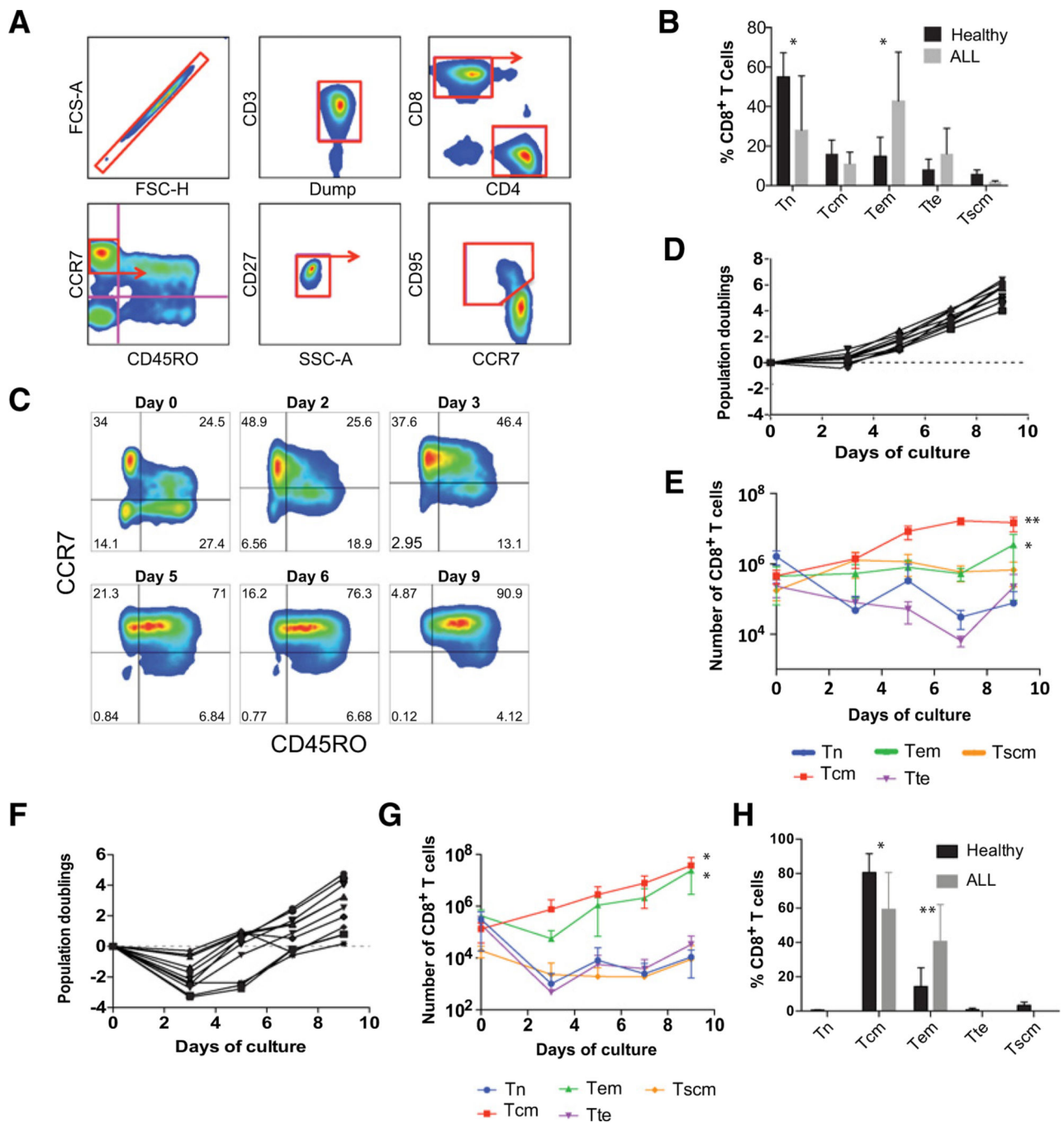
## References

1. Brentjens RJ, Davila ML, Riviere I, Park J, Wang X, Cowell LG, et al. CD19-targeted T cells rapidly induce molecular remissions in adults with chemotherapy-refractory acute lymphoblastic leukemia. *Sci Transl Med* 2013;5:177ra38.
2. Grupp SA, Kalos M, Barrett D, Aplenc R, Porter DL, Rheingold SR, et al. Chimeric antigen receptor-modified T cells for acute lymphoid leukemia. *N Engl J Med* 2013;368:1509–18. [PubMed: 23527958]
3. Kalos M, Levine BL, Porter DL, Katz S, Grupp SA, Bagg A, et al. T cells with chimeric antigen receptors have potent antitumor effects and can establish memory in patients with advanced leukemia. *Sci Transl Med* 2011; 3:95ra73.
4. Maude SL, Frey N, Shaw PA, Aplenc R, Barrett DM, Bunin NJ, et al. Chimeric antigen receptor T cells for sustained remissions in leukemia. *N Engl J Med* 2014;371:1507–17. [PubMed: 25317870]
5. Porter DL, Levine BL, Kalos M, Bagg A, June CH. Chimeric antigen receptor-modified T cells in chronic lymphoid leukemia. *N Engl J Med* 2011; 365:725–33. [PubMed: 21830940]
6. Porter DL, Hwang WT, Frey NV, Lacey SF, Shaw PA, Loren AW, et al. Chimeric antigen receptor T cells persist and induce sustained remissions in relapsed refractory chronic lymphocytic leukemia. *Sci Transl Med* 2015;7:303ra139.
7. Ali SA, Shi V, Maric I, Wang M, Stroncek DF, Rose JJ, et al. T cells expressing an anti-B-cell maturation antigen chimeric antigen receptor cause remissions of multiple myeloma. *Blood* 2016;128:1688–700. [PubMed: 27412889]
8. Fesnak AD, June CH, Levine BL. Engineered T cells: the promise and challenges of cancer immunotherapy. *Nat Rev Cancer* 2016;16:566–81. [PubMed: 27550819]
9. Rapoport AP, Stadtmauer EA, Binder-Scholl GK, Goloubeva O, Vogl DT, Lacey SF, et al. NY-ESO-1-specific TCR-engineered T cells mediate sustained antigen-specific antitumor effects in myeloma. *Nat Med* 2015;21:914–21. [PubMed: 26193344]
10. Tawara I, Kageyama S, Miyahara Y, Fujiwara H, Nishida T, Akatsuka Y, et al. Safety and persistence of WT1-specific T-cell receptor gene-transduced lymphocytes in patients with AML and MDS. *Blood* 2017;130:1985–94. [PubMed: 28860210]

11. O'Rourke DM, Nasrallah MP, Desai A, Melenhorst JJ, Mansfield K, Morrisette JJD, et al. A single dose of peripherally infused EGFRvIII-directed CAR T cells mediates antigen loss and induces adaptive resistance in patients with recurrent glioblastoma. *Sci Transl Med* 2017;9.
12. Heczey A, Louis CU, Savoldo B, Dakhova O, Durett A, Grilley B, et al. CAR T cells administered in combination with lymphodepletion and PD-1 inhibition to patients with neuroblastoma. *Mol Ther* 2017;25: 2214–24. [PubMed: 28602436]
13. Beatty GL, Haas AR, Maus MV, Torigian DA, Soulen MC, Plesa G, et al. Mesothelin-specific chimeric antigen receptor mRNA-engineered T cells induce anti-tumor activity in solid malignancies. *Cancer Immunol Res* 2014;2:112–20. [PubMed: 24579088]
14. Louis CU, Savoldo B, Dotti G, Pule M, Yvon E, Myers GD, et al. Antitumor activity and long-term fate of chimeric antigen receptor-positive T cells in patients with neuroblastoma. *Blood* 2011;118:6050–6. [PubMed: 21984804]
15. Robbins PF, Morgan RA, Feldman SA, Yang JC, Sherry RM, Dudley ME, et al. Tumor regression in patients with metastatic synovial cell sarcoma and melanoma using genetically engineered lymphocytes reactive with NY-ESO-1. *J Clin Oncol* 2011;29:917–24. [PubMed: 21282551]
16. Maude SL, Teachey DT, Porter DL, Grupp SA. CD19-targeted chimeric antigen receptor T-cell therapy for acute lymphoblastic leukemia. *Blood* 2015;125:4017–23. [PubMed: 25999455]
17. Kochenderfer JN, Somerville RP, Lu T, Shi V, Bot A, Rossi J, et al. Lymphoma remissions caused by anti-CD19 chimeric antigen receptor T cells are associated with high serum interleukin-15 levels. *J Clin Oncol* 2017; 35:1803–13. [PubMed: 28291388]
18. Gattinoni L, Klebanoff CA, Restifo NP. Paths to stemness: building the ultimate antitumor T cell. *Nat Rev Cancer* 2012;12:671–84. [PubMed: 22996603]
19. Gattinoni L, Lugli E, Ji Y, Pos Z, Paulos CM, Quigley MF, et al. A human memory T cell subset with stem cell-like properties. *Nat Med* 2011;17: 1290–7. [PubMed: 21926977]
20. Klebanoff CA, Gattinoni L, Torabi-Parizi P, Kerstann K, Cardones AR, Finkelstein SE, et al. Central memory self/tumor-reactive CD8 $\beta$  T cells confer superior antitumor immunity compared with effector memory T cells. *Proc Natl Acad Sci USA* 2005;102:9571–6. [PubMed: 15980149]
21. Wang X, Wong CW, Urak R, Taus E, Aguilar B, Chang WC, et al. Comparison of naive and central memory derived CD8+ effector cell engraftment fitness and function following adoptive transfer. *Oncoimmunology* 2016;5:e1072671.
22. Berger C, Jensen MC, Lansdorp PM, Gough M, Elliott C, Riddell SR. Adoptive transfer of effector CD8+ T cells derived from central memory cells establishes persistent T cell memory in primates. *J Clin Invest* 2008;118:294–305. [PubMed: 18060041]
23. Graef P, Buchholz VR, Stemmerger C, Flossdorf M, Henkel L, Schiemann M, et al. Serial transfer of single-cell-derived immunocompetence reveals stemness of CD8 $\beta$  central memory T cells. *Immunity* 2014;41:116–26. [PubMed: 25035956]
24. Hinrichs CS, Borman ZA, Gattinoni L, Yu Z, Burns WR, Huang J, et al. Human effector CD8+ T cells derived from naive rather than memory subsets possess superior traits for adoptive immunotherapy. *Blood* 2011;117:808–14. [PubMed: 20971955]
25. Hinrichs CS, Borman ZA, Cassard L, Gattinoni L, Spolski R, Yu Z, et al. Adoptively transferred effector cells derived from naive rather than central memory CD8+ T cells mediate superior antitumor immunity. *Proc Natl Acad Sci USA* 2009;106:17469–74. [PubMed: 19805141]
26. Oliveira G, Ruggiero E, Stanghellini MT, Cieri N, D'Agostino M, Fronza R, et al. Tracking genetically engineered lymphocytes long-term reveals the dynamics of T cell immunological memory. *Sci Transl Med* 2015;7: 317ra198.
27. Durek P, Nordström K, Gasparoni G, Salhab A, Kressler C, de Almeida M, et al. Epigenomic profiling of human CD4+ T cells supports a linear differentiation model and highlights molecular regulators of memory development. *Immunity* 2016;45:1148–61. [PubMed: 27851915]
28. Mazo IB, Honczarenko M, Leung H, Cavanagh LL, Bonasio R, Weninger W, et al. Bone marrow is a major reservoir and site of recruitment for central memory CD8 $\beta$  T cells. *Immunity* 2005;22:259–70. [PubMed: 15723813]
29. Parretta E, Cassese G, Barba P, Santoni A, Guardiola J, Di Rosa F. CD8 cell division maintaining cytotoxic memory occurs predominantly in the bone marrow. *J Immunol* 2005;174:7654–64. [PubMed: 15944266]

30. Pulle G, Vidric M, Watts TH. IL-15-dependent induction of 4-1BB promotes antigen-independent CD8 memory T cell survival. *J Immunol* 2006;176:2739–48. [PubMed: 16493029]
31. Zaid A, Mackay LK, Rahimpour A, Braun A, Veldhoen M, Carbone FR, et al. Persistence of skin-resident memory T cells within an epidermal niche. *Proc Natl Acad Sci USA* 2014;111:5307–12. [PubMed: 24706879]
32. Milone MC, Fish JD, Carpenito C, Carroll RG, Binder GK, Teachey D, et al. Chimeric receptors containing CD137 signal transduction domains mediate enhanced survival of T cells and increased antileukemic efficacy in vivo. *Mol Ther* 2009;17:1453–64. [PubMed: 19384291]
33. Porter DL, Levine BL, Bunin N, Stadtmauer EA, Luger SM, Goldstein S, et al. A phase 1 trial of donor lymphocyte infusions expanded and activated ex vivo via CD3/CD28 costimulation. *Blood* 2006;107:1325–31. [PubMed: 16269610]
34. Carpenito C, Milone MC, Hassan R, Simonet JC, Lakhali M, Suhoski MM, et al. Control of large, established tumor xenografts with genetically retargeted human T cells containing CD28 and CD137 domains. *Proc Natl Acad Sci USA* 2009;106:3360–5. [PubMed: 19211796]
35. O'Connor RS, Hao X, Shen K, Bashour K, Akimova T, Hancock WW, et al. Substrate rigidity regulates human T cell activation and proliferation. *J Immunol* 2012;189:1330–9. [PubMed: 22732590]
36. Lugli E, Gattinoni L, Roberto A, Mavilio D, Price DA, Restifo NP, et al. Identification, isolation and in vitro expansion of human and nonhuman primate T stem cell memory cells. *Nat Protoc* 2013;8:33–42. [PubMed: 23222456]
37. Haining WN, Neuberg DS, Keczkemethy HL, Evans JW, Rivoli S, Gelman R, et al. Antigen-specific T-cell memory is preserved in children treated for acute lymphoblastic leukemia. *Blood* 2005;106:1749–54. [PubMed: 15920008]
38. Singh N, Perazzelli J, Grupp SA, Barrett DM. Early memory phenotypes drive T cell proliferation in patients with pediatric malignancies. *Sci Transl Med* 2016;8:320ra3.
39. Barrett DM, Singh N, Liu X, Jiang S, June CH, Grupp SA, et al. Relation of clinical culture method to T-cell memory status and efficacy in xenograft models of adoptive immunotherapy. *Cytotherapy* 2014;16:619–30. [PubMed: 24439255]
40. Klebanoff CA, Scott CD, Leonardi AJ, Yamamoto TN, Cruz AC, Ouyang C, et al. Memory T cell-driven differentiation of naive cells impairs adoptive immunotherapy. *J Clin Invest* 2016;126:318–34. [PubMed: 26657860]
41. Crompton JG, Sukumar M, Roychoudhuri R, Clever D, Gros A, Eil RL, et al. Akt inhibition enhances expansion of potent tumor-specific lymphocytes with memory cell characteristics. *Cancer Res* 2015;75:296–305. [PubMed: 25432172]
42. van der Waart AB, van de Weem NM, Maas F, Kramer CS, Kester MG, Falkenburg JH, et al. Inhibition of Akt signaling promotes the generation of superior tumor-reactive T cells for adoptive immunotherapy. *Blood* 2014;124:3490–500. [PubMed: 25336630]
43. Gattinoni L, Zhong X-S, Palmer DC, Ji Y, Hinrichs CS, Yu Z, et al. Wnt signaling arrests effector T cell differentiation and generates CD8+ memory stem cells. *Nat Med* 2009;15:808–13. [PubMed: 19525962]
44. Muralidharan S, Hanley PJ, Liu E, Chakraborty R, Bollard C, Shpall E, et al. Activation of Wnt signaling arrests effector differentiation in human peripheral and cord blood-derived T lymphocytes. *J Immunol* 2011;187: 5221–32. [PubMed: 22013128]
45. Lu TL, Pugach O, Somerville R, Rosenberg SA, Kochenderfer JN, Better M, et al. A rapid cell expansion process for production of engineered autologous CAR-T cell therapies. *Hum Gene Ther Methods* 2016;27:209–18. [PubMed: 27897048]
46. Schmueck-Henneresse M, Omer B, Shum T, Tashiro H, Mamonkin M, Lapteva N, et al. Comprehensive approach for identifying the T cell subset origin of CD3 and CD28 antibody-activated chimeric antigen receptor-modified T cells. *J Immunol* 2017;199:348–62. [PubMed: 28550199]
47. Kagoya Y, Nakatsugawa M, Ochi T, Cen Y, Guo T, Anczurowski M, et al. Transient stimulation expands superior antitumor T cells for adoptive therapy. *JCI Insight* 2017;2:e89580.

48. Neelapu SS, Tummala S, Kebriaei P, Wierda W, Gutierrez C, Locke FL, et al. Chimeric antigen receptor T-cell therapy—assessment and management of toxicities. *Nat Rev Clin Oncol* 2018;15:47–62. [PubMed: 28925994]
49. Ahmed N, Brawley V, Hegde M, Bielaowicz K, Kalra M, Landi D, et al. HER2-specific chimeric antigen receptor-modified virus-specific T cells for progressive glioblastoma: a phase 1 dose-escalation trial. *JAMA Oncol* 2017;3:1094–101. [PubMed: 28426845]
50. Brown CE, Alizadeh D, Starr R, Weng L, Wagner JR, Naranjo A, et al. Regression of glioblastoma after chimeric antigen receptor T-cell therapy. *N Engl J Med* 2016;375:2561–9. [PubMed: 28029927]
51. Tanyi JL, Haas AR, Beatty GL, Stashwick CJ, O'Hara MH, Morgan MA, et al. Anti-mesothelin chimeric antigen receptor T cells in patients with epithelial ovarian cancer. *J Clin Oncol* 2016;34(no. 15\_suppl):5511.
52. Lam N, Alabanza L, Trinklein N, Buelow B, Kochenderfer JN. T cells expressing anti-B-cell maturation antigen (BCMA) chimeric antigen receptors with antigen recognition domains made up of only single human heavy chain variable domains specifically recognize Bcma and eradicate tumors in mice. *Blood* 2017;130:504.
53. Fraietta J, Lacey S, Orlando E, Pruteanu-Malinici I, Gohil M, Lundh S, et al. Determinants of response and resistance to CD19 chimeric antigen receptor (CAR) T cell therapy of chronic lymphocytic leukemia. *Nat Med* 2018;24:563–71. [PubMed: 29713085]
54. Guidance for Industry, U.S. Department of Health and Human Services, Food and Drug Administration, Center for Biologics Evaluation and Research (CBER). Supplemental guidance on testing for replication-competent retrovirus in retroviral vector-based gene therapy products and during follow-up of patients in clinical trials using retroviral vectors. *Hum Gene Ther* 2001;12:315–20. [PubMed: 11177567]
55. Couzin-Frankel J. Supply of promising T cell therapy is strained. *Science* 2017;356:1112–3. [PubMed: 28619895]

**Figure 1.**

T cells progressively differentiate over time during *ex vivo* culture. **A**, Gating strategy used to identify Tn, Tscm, Tcm, Tem, and Tte subsets. The arrow identifies which subset was examined further. **B**, The proportion of CD8<sup>+</sup> T-cell subsets freshly isolated from the peripheral blood of healthy donors ( $n = 9$ ) and individuals with ALL ( $n = 9$ ) calculated using the gating strategy shown in **A**. \*,  $P < 0.05$ . **C**, Representative plots of CART19 cells at the specified timepoints during culture. Pregated for live CD3<sup>+</sup>CD8<sup>+</sup> T cells as shown in **A**. **D**, *Ex vivo* proliferation of healthy donor T cells following stimulation with anti-CD3/CD28



microbeads. Total viable T cells were enumerated by flow cytometry using bead-based counting. Each donor is represented by a separate line. Dotted line: 0 population doublings. **E**, Absolute counts of CD8<sup>+</sup> T cells subsets over time in cultures of healthy donors shown in **D**. Data are plotted as mean  $\pm$  SD. \*\*,  $P < 0.01$ ; \*,  $P < 0.05$  comparing d3 vs. d9. **F**, *Ex vivo* proliferation of T cells from ALL patients stimulated and enumerated as in **D**. **G**, Absolute counts of CD8<sup>+</sup> T cells from ALL patients as shown in **F**. \*,  $P < 0.05$ ; \*\*,  $P < 0.05$  comparing d3 vs. d9. **H**, The proportion of CD8<sup>+</sup> T cells in healthy donors and ALL patients analyzed on day 9 of culture \*,  $P < 0.05$ ; \*\*,  $P < 0.01$ . All comparisons were analyzed by Wilcoxon matched-pairs signed rank test.

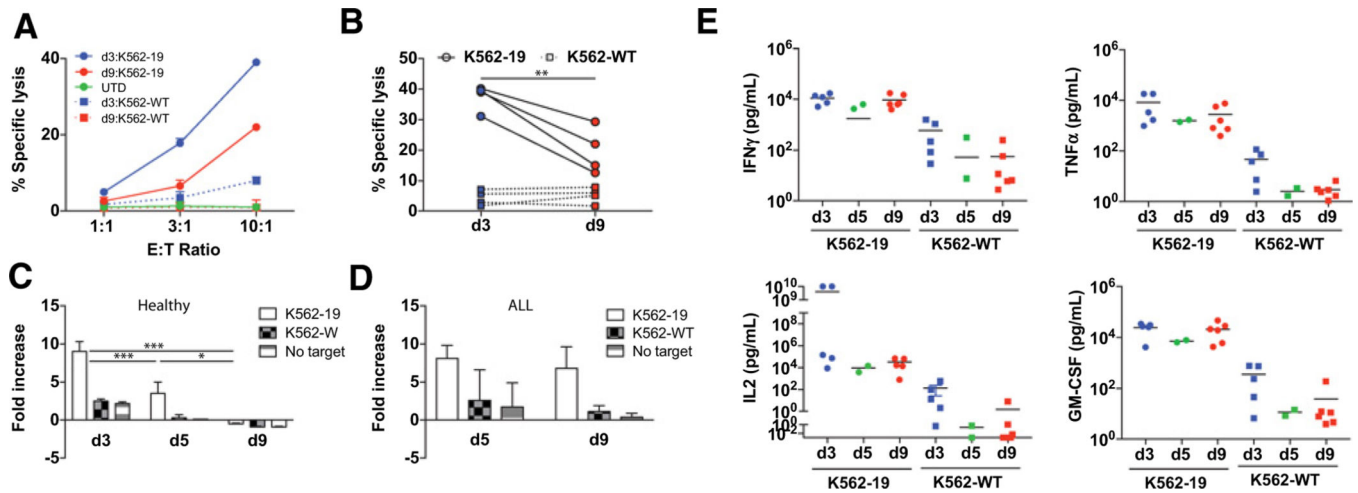


**Figure 2.**

Early-harvested CART19 cells show enhanced effector function and proliferation following antigen exposure *in vitro*. **A**,  $^{51}\text{Cr}$  release after 4 hours of CART19 cells harvested on days 3 and 9 when cocultured at the indicated E:T ratio with CD19-expressing K562 cells (K562–19) or wild-type K562 (K562-wild type) to measure specific cytotoxicity. Mean values of triplicate culture are shown. **B**, Similar results were obtained in an independent experiment from different healthy donors ( $n = 4$ ) at a 10:1 E:T ratio. \*\*,  $P < 0.01$  d3 vs. d9. **C**, CFSE-labeled CART19 cells from healthy donors ( $n = 3$ ) expanded and harvested on days 3, 5, and 9 were cocultured with K562–19, K562-wild type, or medium only for 120 hours at a 1:1 E:T ratio. Relative fold change of live T-cell count normalized to T-cell count at day 0 is shown. Data are plotted as mean  $\pm$  SD. \*\*\*,  $P < 0.001$  comparing d3 vs. d5 and d9; \*,  $P < 0.05$  comparing d5 vs. d9. **D**, CFSE-labeled CART19 cells from individuals with ALL ( $n = 3$ ) were expanded and analyzed as in **C**. **E**, CART19 cells from healthy donors ( $n = 5$ ) were cocultured with K562–19 cells or K562-wild type for 24 hours at a 1:1 E:T ratio. Supernatants were collected after 24 hours. Cytokines were measured by Luminex analysis. Horizontal black line: mean of each group.

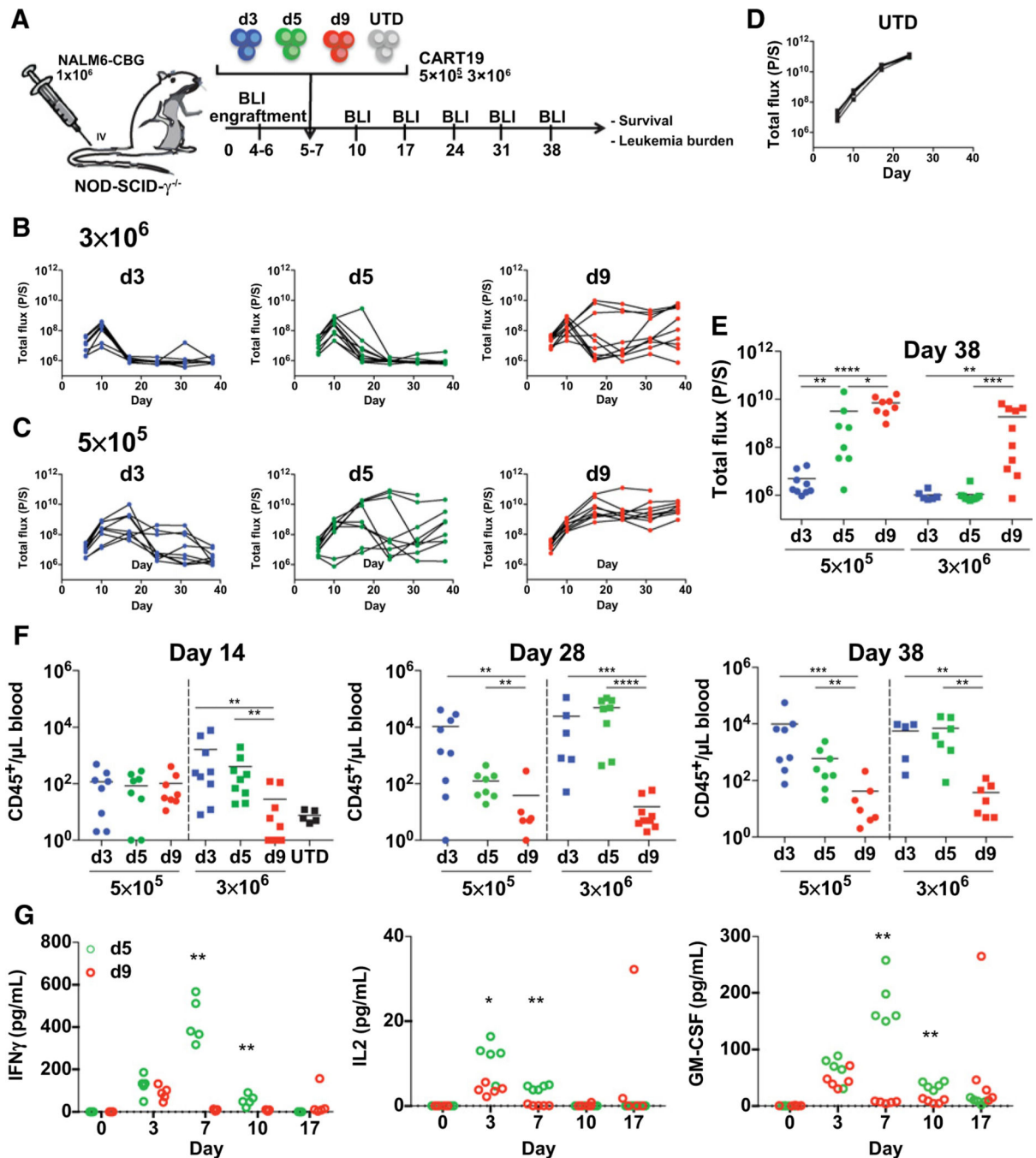


**Figure 3.**

Early-harvested CART19 cells show more potent and durable antitumor responses *in vivo*. **A**, Schematic of the xenograft model and CART19 cell treatment (derived from healthy donors) in NSGs i.v. injected with  $1 \times 10^6$  NALM6 cells. Day 3, 5, and 9 CART19 cells or control T cells (UTD) were i.v.-injected in mice 5 to 7 days after NALM6 injection ( $n = 9$ ). **B** and **C**, Serial quantification of disease burden by bioluminescence imaging. **(B)** A high ( $3 \times 10^6$ ) and **(C)** a low ( $5 \times 10^5$ ) dose of CART19 cells were selected to examine the antitumor cytolytic activity of day 3, 5, and 9 CART19 cells. **D**, Disease progression in mice

treated with UTD control T cells ( $n = 5$ ). **E**, Quantification of tumor burden by bioluminescence imaging on day 38 in mice treated with CART19 cells harvested at the indicated times. Symbols represent one mouse each. Horizontal black line: mean of each group. **F**, Absolute peripheral blood CD45<sup>+</sup> T-cell counts every 2 weeks after CART19 cell or UTD cell injection and at the end of the experiment (day 38) measured by a TruCount assay. **G**, Using an experimental design as described in panel, day 5 or day 9 CART19 cells were injected into Nalm6-bearing NSG mice. Blood was collected by retro-orbital bleed on the indicated days, and serum human cytokines were analyzed by luminex. Unpaired Mann-Whitney test, two-tailed was used. \*,  $P < 0.05$ ; \*\*,  $P < 0.01$ ; \*\*\*,  $P < 0.001$ ; and \*\*\*\*,  $P < 0.0001$ .

Author Manuscript

Author Manuscript

Author Manuscript

Author Manuscript

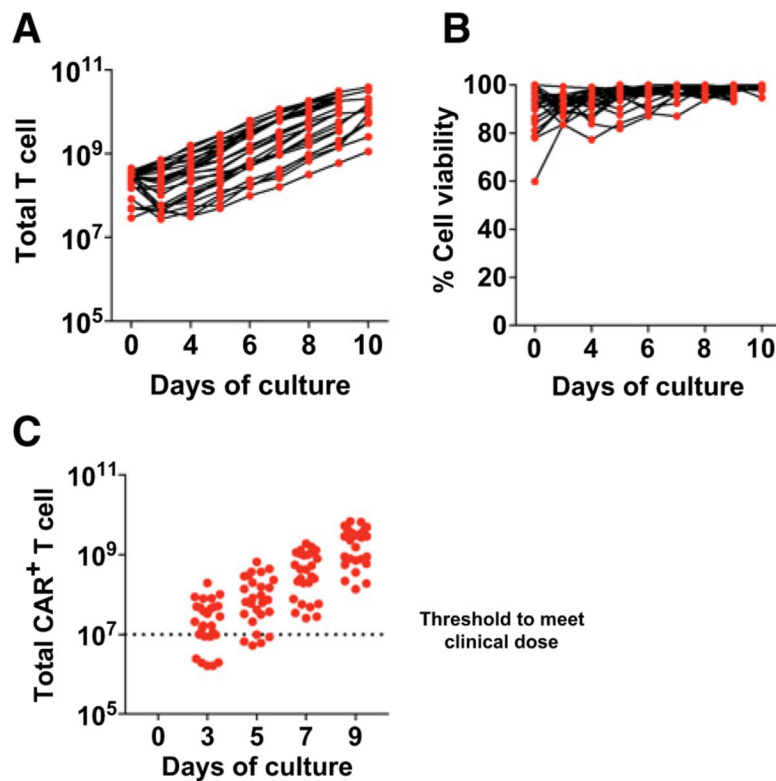


**Figure 4.**

An abbreviated CAR T culture approach is technically feasible in a GMP large-scale production facility. **A**, T cells from ALL patients were stimulated with anti-CD3/CD28 microbeads and expanded *ex vivo* using a large-scale cGMP process as described in the Materials and Methods. Activated T cells were transduced with CD19-BB $\zeta$  CAR. Total T-cell number during expansion is shown ( $n = 27$  independent patients). **B**, T-cell viability was assessed by flow cytometry over time for the patients in **A**. **C**, CD19-CAR abundance was measured by qPCR at days 3, 5, 7, and 9 of expansion. The target dose of day 9 CAR<sup>+</sup> T cells for clinical applications is represented by the dotted line.

**Table 1.**

## ALL donor characteristics

<b>Donor</b>	<b>Age</b>	<b>Sex</b>	<b>Disease specified in clinical protocol</b>
#1	57	Female	Resistant or refractory B-cell ALL
#2	50	Male	Resistant or refractory B-cell ALL
#3	43	Male	Resistant or refractory B-cell ALL
#4	4	Male	Pediatric relapsed and refractory B-cell ALL
#5	18	Male	Pediatric relapsed and refractory B-cell ALL
#6	12	Female	Pediatric relapsed and refractory B-cell ALL
#7	16	Female	Pediatric relapsed and refractory B-cell ALL
#8	17	Male	Pediatric relapsed and refractory B-cell ALL
#9	14	Male	Pediatric relapsed and refractory B-cell ALL

Author Manuscript

Author Manuscript

Author Manuscript

Author Manuscript